

Geometrically Realizing Nested Torus Links

Amie Bray

August 18, 2017

Abstract

In this paper, we define nested torus links. We then go on to introduce a cell decomposition of nested torus links. Using the cell decomposition and its resulting circle packing we prove that nested torus links can be geometrically realized via regular ideal octahedra in hyperbolic space.

1 Introduction

A link is hyperbolic if and only if its complement admits a complete hyperbolic structure. This means the complement must admit a metric of constant curvature -1 . Hyperbolic polyhedra provide another way to describe hyperbolic structures on link complements. Starting with the link complement, one can find a cell decomposition slicing the link complement, so to define edges and faces of an ideal polyhedron in hyperbolic space. We then invoke Andreev's Theorem to result in a circle packing associated with the ideal polyhedra.

Cell decomposition is a way of assigning 0, 1, 2, and 3 cells such that 0-cells have no dimension, 1-cells are in one dimension, 2-cells are 2-dimensional, and 3 cells are 3-dimensional. Cutting along 2-cells determines the faces of the 3-cells, which become the ideal polyhedra in \mathbb{H}^3 . A cell decomposition, together with gluing instructions, realizing a link complement as hyperbolic must satisfy Poincaré's Polyhedral Theorem, see [1]. In [3], Champanerkar, et al use a tetrahedral decomposition to determine volume bounds for Dehn fillings of nested torus links -called twisted torus links. Here we seek to better understand the geometry of nested torus links by proving they have an octahedral geometric realization. The proof of Theorem 3 in [4] says if that we can recognize an octahedral cell decomposition by looking at its resulting circle packing.

1.1 Torus Links

Before defining nested torus links, we introduce torus links and their notation. Torus links are those which lie on the surface of an unknotted torus in 3-Space, such that there are no self-intersections of the link on the surface of the torus. Such links are classified with the notation (p, q) , where p is the number of times the link completes a

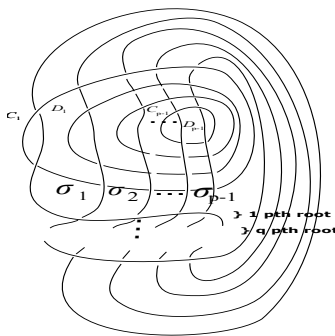


Figure 1: The $\tilde{\delta}_p^q$ nested torus link

full revolution around the longitude of the torus, and q is the number of times the link winds around the meridian. Note that with a simple isotopy of the torus, the (p, q) link is equivalent to the (q, p) . The number of components of the (p, q) link is the $gcd(p, q)$, see [2]. Thus when p and q are coprime, the link is of one component - a true torus knot.

Following the notation from [3], torus links are realized as closed braids having the form

$$(\sigma_1 \sigma_2 \cdots \sigma_{p-1})^q$$

where $\delta_p = \sigma_1 \sigma_2 \cdots \sigma_{p-1}$ is a p th root of the full twist, Δ_p^2 , of p strands. Note that $\delta_p^p = \Delta_p^2$.

2 Nested Torus Links

Nested torus links are the result of adding $p-1$ crossing circles, C_1, C_2, \dots, C_{p-1} over the (p, q) link such that C_1 encompasses the entire closed braid, C_2 encompasses the right most $p-1$ strands, and so on, until C_{p-1} crosses over only the two right most strands, see Figure 1. As a convention, we will always nest in this way - so that the inner most crossing circle encompasses only the right most strands. The closed braid word for the (p, q) torus link is δ_p^q , so to differentiate between the torus link and its nested partner, the notation for a nested (p, q) torus link will hereafter be $\tilde{\delta}_p^q$.

Associated to each crossing circle C_k is a crossing disk, D_k , perpendicular to the plane of projection. For simplicity, let all D_k be coplanar. It is important to note that D_k is a thrice-punctured sphere. The inner most crossing disk, D_{p-1} is punctured twice by knot strands and once by the crossing circle C_{p-1} . In general, D_k is punctured by a single knot strand, C_{k-1} , and C_k . Figure 1 demonstrates a general $\tilde{\delta}_p^q$.

2.1 Homeomorphisms and Equivalence of Nested Torus Links

Our ultimate goal is to show nested torus links are octahedral. Because isotopic and homeomorphic links have the same geometric structure, we use them to restrict the

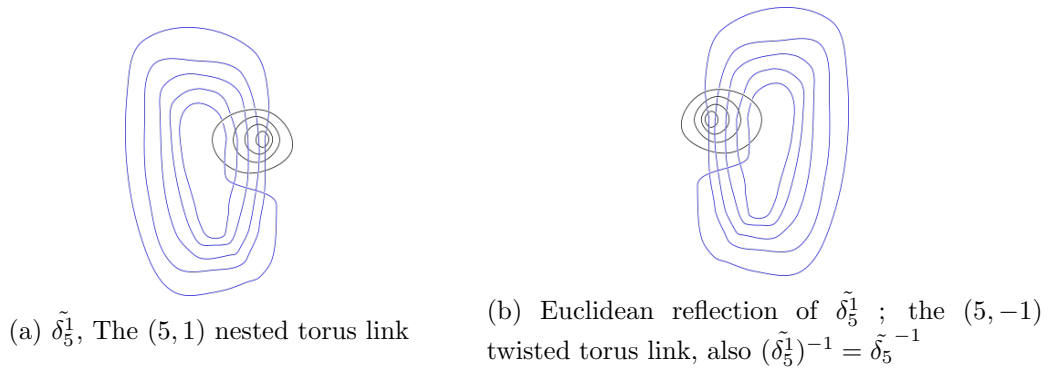


Figure 2: Equivalence of links via Euclidean Reflection

number of cases we need to consider. There are certain allowable moves to describe an equivalence via homeomorphism between nested torus links.

Reflection

Reflection is a true Euclidean isometry. Therefore if there exists a reflection between two nested torus links over a plane in the embedding space (\mathbb{R}^3), then the two nested torus links are homeomorphic. Figure 2 shows that $(p, q) \equiv (p, -q)$, or in braid notation:

$$\tilde{\delta}_p^q = (\sigma_1 \sigma_2 \cdots \sigma_{p-1})^q \equiv (\sigma_1 \sigma_2 \cdots \sigma_{p-1})^{-q} = \tilde{\delta}_p^{-q}$$

where $\tilde{\delta}_p^q$ is nested on the right and $\tilde{\delta}_p^{-q}$ is nested on the left.

Isotopies

Two links are isotopic if one can simply pull the strands of the first link so that it coincides with the second, without cutting, gluing, or changing the sign of crossings. These are used to define topological equivalence between links.

Full Twists

In the discussion of fully augmented links, it is known that slicing along crossing disks and regluing with a full twist yields homeomorphic links. In the case of nested torus links, the same is true over any given crossing disk. Full twists are in the form $\tilde{\delta}_p^p$, or (p, p) . Therefore, given a nested full twist, $\tilde{\delta}_p^p$, we can apply the homeomorphism in which the inverse of a full twist is inserted:

$$\begin{aligned} \tilde{\delta}_p^p \tilde{\delta}_p^{-p} &= (\sigma_1 \sigma_2 \cdots \sigma_{p-1})^p \cdot (\sigma_1 \sigma_2 \cdots \sigma_{p-1})^{-p} \\ &= (\sigma_1 \sigma_2 \cdots \sigma_{p-1})^0 \\ &= \tilde{\delta}_p^0 \end{aligned}$$

In the above notation, we see that inserting the inverse of a full twist to a full twist undoes each of the crossings in the braid. Generally, this means $\tilde{\delta}_p^0 \equiv \tilde{\delta}_p^p$. Furthermore, we can undo any existing full twist in a given $\tilde{\delta}_p^q$ nested torus link. Therefore, we know $\tilde{\delta}_p^q \equiv \tilde{\delta}_p^{q \bmod p}$. Consequently, let $q < p$ for $\tilde{\delta}_p^q$.

Lemma 2.1. *Up to homeomorphism, for $\tilde{\delta}_p^q$, $0 < q \leq p/2$.*

Proof. We show this by proving if $q + z = 0 \pmod{p}$, then $\tilde{\delta}_p^q$ and $\tilde{\delta}_p^z$ are homeomorphic. Recall that $q + z = 0 \pmod{p}$ if and only if $q + z = np$ for some n .

Starting with $\tilde{\delta}_p^q = (\sigma_1 \sigma_2 \cdots \sigma_{p-1})$, apply the inverse of a full twist n times. This is the composition of n full twist homeomorphisms, so it is itself a full twist homeomorphism. Thus we have:

$$\tilde{\delta}_p^q \equiv \delta_p^{q-np}$$

But $q - np = -z$, so we have

$$\tilde{\delta}_p^q \equiv \delta_p^{q-np} \equiv \delta_p^{-z} \equiv \tilde{\delta}_p^z$$

The homeomorphism from $\tilde{\delta}_p^{-z}$ to $\tilde{\delta}_p^z$ is a reflection. □

3 Cell Decomposition

Throughout this section, we prove that nested torus links, $\tilde{\delta}_p^q$ are octahedral for $p \geq 3$ and $q \geq 1$.

Note that $\tilde{\delta}_p^0$ contains an embedded annulus, regardless of p , and is thus not hyperbolic. Additionally if, $p < 3$, Lemma 2.1 says $q \leq 1$. If $q = 0$, then the link is clearly not hyperbolic. But when $p < 3$ and $q = 1$, the link also contains an embedded annulus and is thus not hyperbolic. Furthermore, up to homeomorphism, proving that nested torus links are octahedral for $1 \leq q \leq p/2$ is sufficient for proving the same result for all $q \geq 1$, by Lemma 2.1.

3.1 Preliminaries

The results from [4] generalize the cell decomposition of a half twist over a single crossing disk, see Figure 4, to one involving multiple strands. In the case of nested torus links, we will again generalize the cell decomposition for a half twist over a single crossing disk, but only over a subset of braid strands. Additionally, we will recall the geometry of Δ_p because it will be illustrative in understanding the geometry of $\tilde{\delta}_p^q$.

Cells

Recall that in cell decomposition, 0-cells are end points for 1-cells, 1-cells bound 2-cells, and 2-cells bound 3-cells. In the case of cell decomposition for fully augmented link complements, we assign 1-cells as the intersection of the crossing disk plane with the plane of projection. The end points of these segments are knot and crossing strands, or punctures in the link complement. Therefore, there are no 0-cells in the manifold; these become ideal vertices in hyperbolic space. The 2-cells are “planar” regions, including twisted bands that live along the plane of projection, and the 3-cells are “space” like regions above and below the plane of projection. The plane of projection splits space so that we have 2 3-cells, P_+ and P_- . The 2-cells bounding P_+ are those visible from

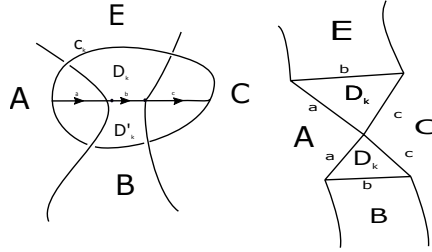


Figure 3: Flattened cell decomposition of an untwisted crossing disk

above. Similarly the 2-cells visible from below are associated with P_- .

Cell Decomposition Over a Single Crossing Disk

Cell decomposition over untwisted crossing disks is well understood, through the discussion of fully augmented links. As usual, there are no 0-cells, the 1-cells are the intersection of the crossing disk with the plane of projection, and there are two 3-cells split by the plane of projection. The 2-cells are determined so that cutting along them yields the boundary faces of the two 3-cells. Figure 3 illustrates that the 3-cell P_+ is bounded by the planar regions, A, B, C , and E , and twice by D_k - once from the front and once from the back. A reflection of the same picture occurs for P_- .

The cell decomposition over a single half-twisted crossing disk, described in [4], is similar to that over an untwisted crossing disk. However, the half twist changes the gluing instructions for 2-cells, as illustrated in Figure 4, so that P_+ is bounded by D'_k on the front and D_k on the back. That is, because of the half twist, D'_k is visible from the 3-cell above the plane of projection. For this reason, it is helpful to look at the 2-cells for P_+ from the front and back separately, keeping gluing instructions consistent. A similar picture describes the cell decomposition on P_- . See [4] for more details.

Cell Decomposition of Nested Half Twists

Let us recall the general structure of such a nested half twist, using the example Δ_5 . Figure 5a illustrates the a half twist over the entire crossing region, composed of the sub crossing disks, E, F, G , and H . Looking at the diagram from the front, consider the inner most punctures of the crossing disk E - a single strand and the outer most puncture of the crossing disk F . There is a half twist over these two punctures. The same is true between the punctures of F, G , and H . That is, there is a half twist on the front side of each crossing disk. Looking at the diagram from the back, each of the crossing disks lay flat. Note that in the gluing instructions for the cell decomposition illustrate this nicely, see Figure 5b. We see E', F', G' , and H' on the front, corresponding to a half twist. On the back, where the two cells are glued flat, we see E, F, G , and H . [4]

Understanding Nested Torus Links

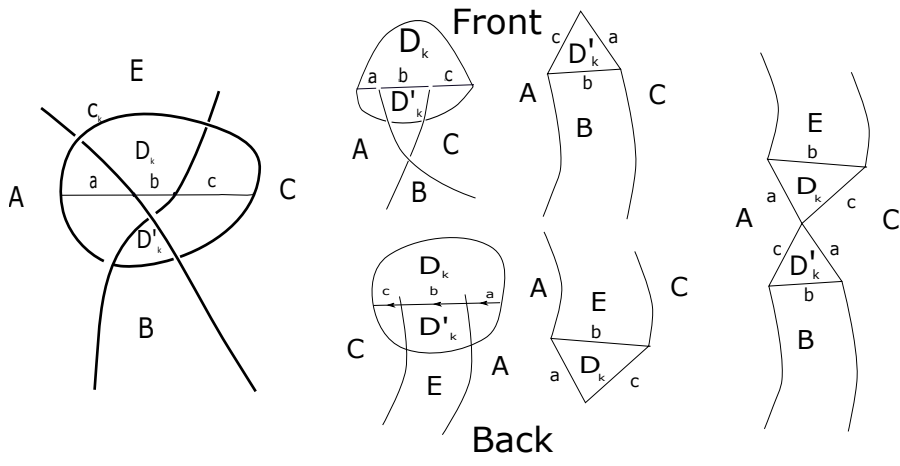


Figure 4: Cell decomposition on a half twisted crossing disk

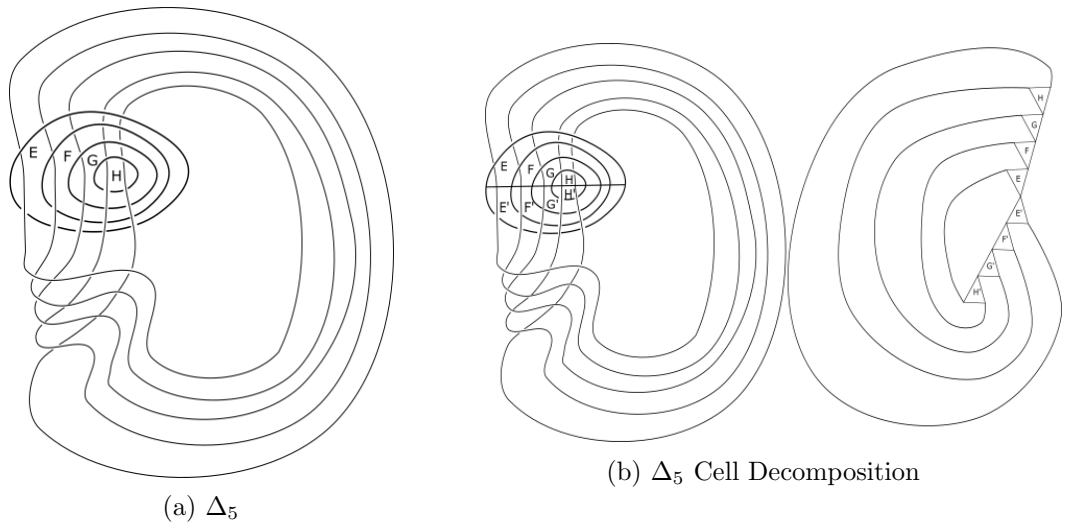


Figure 5: Understanding the Δ_5 link

In order to apply the cell decomposition of half twisted crossing disks to the more general case of the nested torus link, we first isotope $\tilde{\delta}_p^q$ so to better describe gluing instructions for 2-cells.

Lemma 3.1. *There is an isotopy of $\tilde{\delta}_p^q$ such that the braid can be viewed as a half-twist over the first q crossing disks on the front, and a half twist over the last $q - 1$ crossing disks on the back.*

Proof. Start with $\tilde{\delta}_p^q$. Note that the sub-braid consisting of the left-most q strands is in the form (q, q) and is thus a full twist. The left q strands cross over the last $p - q$ strands, so that the left q strands end up the right q strands on the back. Isotope the last half of the full twist on the left q strands around to the back of the crossing disks. On this side, this represents a half twist over the last q strands. Because the last two strands puncture only the inner most crossing disk, this corresponds to a half-twist over the last $q - 1$ crossing disks on the back. Figure 6 demonstrates this isotopy for $\tilde{\delta}_5^2$, and the general $\tilde{\delta}_p^q$. \square

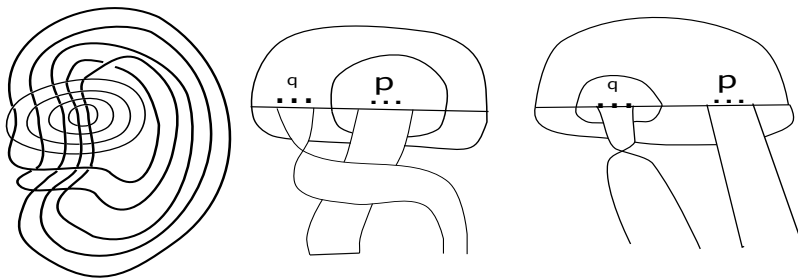


Figure 6: Left: The $\tilde{\delta}_5^2$ nested link after the isotopy from Lemma 3.2. Middle: The front copy of $\tilde{\delta}_p^q$ after Lemma 3.2. Right: The back copy of $\tilde{\delta}_p^q$ after the same isotopy.

3.2 Nested Torus Cell Decomposition

Theorem 3.2. *The nested torus link, $\tilde{\delta}_p^q$ is octahedral for $p \geq 3$ and $q \geq 1$*

Proof. As aforementioned, Lemma 3.1 results in Figure 6. Because we are dealing with half twisted crossing disks, it is helpful to use this picture to determine the cell decomposition for $\tilde{\delta}_p^q$, keeping consistent gluing instructions. Additionally, we look at the cell decomposition of P_+ . The proof for P_- is analogous.

1-Cells Because each crossing disk is a thrice punctured sphere, the resulting cell decomposition will have an even number of triangular crossing disk faces, each bounded by 1-cells. The 1-cells bounding crossing disk D_k are denoted a_k^1, a_k^2 , and a_k^3 . For all

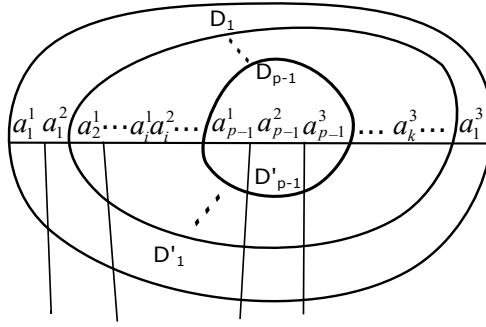


Figure 7: 1-cells of $\tilde{\delta}_p^q$.

values of k , a_k^3 is to the right of the closed braid because of nesting. See Figure 7.

2-Cells First perform the isotopy from Lemma 3.1. The 2-cells are determined by grouping like strands on half-twisted bands, and considering the front and back separately. See labels W, X, Y and Z in Figure 8. Regions containing many knot strands decompose into many separate 2-cells. The half-twisted band, denoted region Y in the Figure 8, contains q strands. As a result, there are $q - 1$ distinct 2-cells grouped together in this region. These are counted by the number of planar spaces between strands. Similarly, the flat band, denoted by region W has $p - q$ strands, and $p - q - 1$ distinct 2-cells within this region. The regions denoted X, V and Z each contain exactly one 2-cell because they are not sliced by knot strands.

Now because all twisting occurs near the crossing disks, away from the crossing disks, all 2-cells lie planar - or untwisted. As we approach crossing disks on the front, the left q strands lie on a half-twisted band; the right $p - q$ strands lie on a flat band. The 2-cells between these bands are as in the case of a single half twist applied to this more general situation.

Note that the first q crossing disks have a half twist over their crossing disks on the front. Therefore, by the cell decomposition described in [4], $D'_1 \cdots D'_q$ are visible from P_+ on the front. On the back, the crossing disks $D'_{q+2} \cdots D'_{p-1}$ are visible from P_+ for the same reason. All other crossing disks are flat. Figure 8 demonstrates regions of two cells, including their gluing instructions over crossing circles.

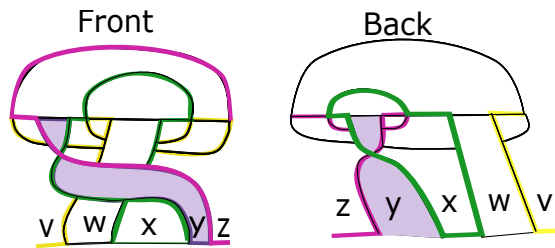


Figure 8: 2-cell regions of $\tilde{\delta}_p^q$.

Flattening the Cell Decomposition Shrinking the crossing strands to ideal vertices results in Figure 9. Note that Region Y contains $q - 1$ 2-cell faces, and Region W contains $p - q - 1$ 2-cell faces, as previously explained. Each of these regions *must*

contain at least one 2-cell bounded by exactly three 1-cells because each region has two strands puncturing the inner most crossing disk. These 2-cells are tangent to exactly three other 2-cells, not including crossing disks.

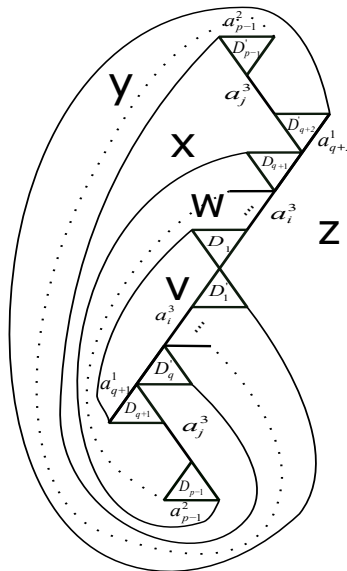


Figure 9: flattened 2-cells of $\tilde{\delta}_p^q$.

Circle Packing Finally, we shrink the knot strands to result in a circle packing, Figure 10. Each 2-cell, not including those from crossing disk shrinks to a circle. The crossing disks shrink to an even number of triangular faces. The 2-cell region Z is tangent to each 2-cell in regions X , W , and V , and only the outermost 2-cell of region Y . This is the outside face of circle packing. The 2-cell in region X is tangent to every other 2-cell, so each circle in the resulting circle packing must be tangent to the circle labeled X . Each region W and Y contains a 2-cell that decomposes to a circle tangent to exactly three other circles, because both regions contain a triangular 2-cell. According to the proof of Theorem 3 in [4], we can recognize a circle packing as octahedral if the it is the result of adding a mutually tangent circle between three existing mutually tangent circles; the corresponding polyhedron is the result of appending an octahedron onto an existing polyhedron. Through this, we see that the resulting circle packing associated to any $\tilde{\delta}_p^q$ corresponds to an ideal polyhedron formed by appending octahedra to an existing polyhedron. Therefore, the link complement for $\tilde{\delta}_p^q$ is octahedral. □

Figure 11 illustrates the octahedral cell decomposition of $\tilde{\delta}_5^2$.

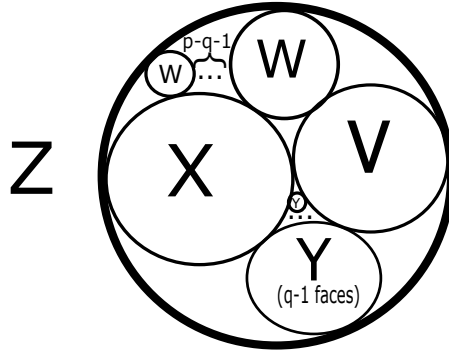


Figure 10: Circle packing associated to $\tilde{\delta}_p^q$.

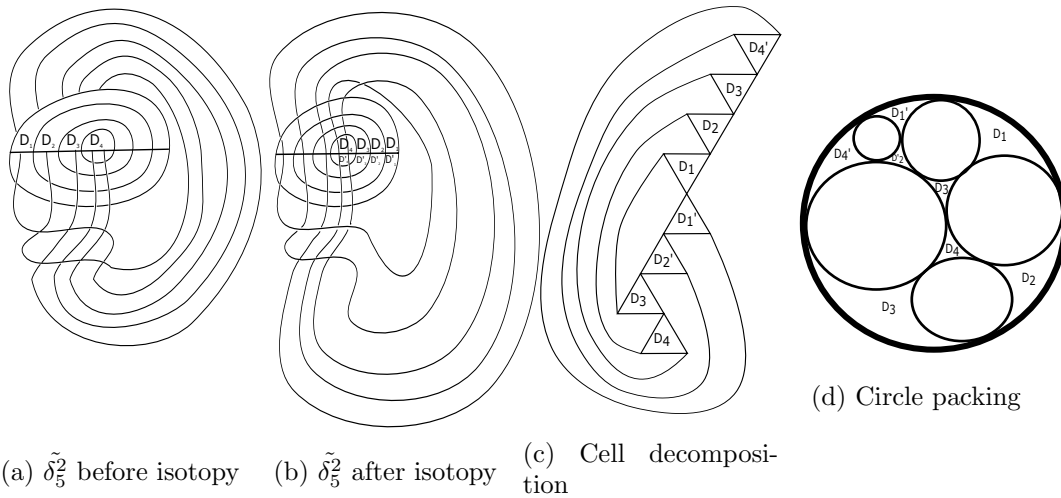


Figure 11: Cell decomposition for $\tilde{\delta}_5^2$

4 Open Questions

How does knowing that nested torus links are octahedral improve volume bounds for their Dehn fillings, twisted torus links?

5 Acknowledgments

I would like to extend a special thanks to Dr. Rolland Trapp for his support and encouragement throughout my exploration of this problem. I would also like to thank Dr. Corey Dunn and Dr. Trapp for their dedication to undergraduate research and their outstanding efforts in sponsoring the California State University San Bernardino REU program. This project was funded both by NSF grant DMS-1461286 and California State University San Bernardino.

References

- [1] F. Bonahon. *Low-Dimensional Geometry: from Euclidean surfaces to hyperbolic knots*, volume 49. American Mathematical Society, 2009.
- [2] M. A. Bush, K. R. French, and J. R. H. Smith. Total linking numbers of torus links and klein links. *Rose-Hulman Undergraduate Mathematics Journal*, 15:72–92, 2014. Published online.
- [3] A. Chamanerkar, D. Futer, I Kofman, W. Neuman, and J. S. Purcell. Volume bounds for generalized twisted torus links. *Mathematical research letters*, 18:1097–1120, 2011.
- [4] J. Harnois, H. Olson, and R Trapp. Hyperbolic tangle surgeries and nested links. preprint.